Differentiation of oxidized low density lipoproteins by nanosensors

Mahsa Rouhanizadeh [a], Tao Tang [b], Chao Li [b], Juliana Hwang [c],
Chongwu Zhou [b], Tzung K. Hsiai [a,*]

[a] *Department of Biomedical Engineering and Division of Cardiovascular Medicine, University of Southern California,
School of Engineering and School of Medicine, Los Angeles, CA 90089-1451, USA*
[b] *Department of Electrical Engineering, Electro-Physics, University of Southern California, School of Engineering,
Los Angeles, CA 90089-1451, USA*
[c] *Department of Molecular Pharmacology and Toxicology and the Atherosclerosis Research Unit,
School of Pharmacy, University of Southern California, USA*

Abstract

Oxidized low density lipoprotein (oxLDL) is considered a biomarker for acute heart attack in patients with coronary artery disease (CAD). LDL cholesterol in the circulatory system can undergo oxidative modification to oxidized LDL (oxLDL), leading to the development of CAD. We tested whether indium oxide (In_2O_3) nanowires network- and carbon nanotube network-based field effect transistors (FETs) were able to differentiate the LDL cholesterol between the reduced (native LDL) and the oxidized state (oxLDL). LDL samples isolated from human plasma were exposed to In_2O_3 FETs, and conductivities and gating characteristics were obtained as current versus drain-source voltage ($I_D–V_{DS}$), and current versus gate-source voltage ($I_D–V_{GS}$). A higher conductivity was observed in the LDL sample containing 15.1% oxLDL relative to the sample containing 4.4% oxLDL. The results were validated by high performance liquid chromatography (HPLC). Next, carbon nanotube network-based FETs conjugated with anti-copper oxLDL antibody were exposed to the LDL samples. Distinct conductivities between nLDL and oxLDL were also observed from the I_D versus time domain curve in the presence of bovine serum albumin (BSA), demonstrating nano-scale sensors as potential lab-on-a-chip devices for detection of oxLDL cholesterol.

1. Introduction

Cardiovascular diseases are the emergent global health issue largely owing to the accelerating prevalence in the developing nations [1]. Oxidized LDL cholesterol (oxLDL) is known to initiate the development of coronary artery disease [2]. Elevated serum level of oxLDL predicts acute heart attack or coronary syndromes [3–5]. High performance liquid chromatography (HPLC) has been the mainstay to fractionate the percentage of oxLDL in LDL samples from the human plasma [6]. However, the development of nano-scale sensors

provides a potential lab-on-chip capability to detect oxLDL cholesterol in a small amount of LDL samples.

Nanowire-based field effect transistors (FETs) have been demonstrated in biochemical applications. The development of nanowires has been based on a family of oxides harboring interesting optical and electrical properties. These binary oxide nanowires include GeO_2, Ga_2O_3, MgO_4 and SiO_2 [7]. Indium oxide (In_2O_3) represents a wide band gap transparent conductor with a direct and indirect band gaps at ∼3.6 and at ∼2.6 eV, respectively [8,9]. This unique property provides a broad spectrum of applications from solar cells to liquid crystal displays [10]. In addition to the application of chemical sensors [11], boron-doped silicon nanowire-based FETs have also been capable of detecting calcium ion (Ca^{2+}) [12]. Also, the tin-doped indium oxide thin film (In_2O_3: Sn, ITO)

* Corresponding author. Tel.: +1 213 740 7236; fax: +1 213 740 0343.
E-mail address: Hsiai@usc.edu (T.K. Hsiai).

has been applied for flat panel displays in biomedical instruments by virtue of its high electrical conductivity and optical transparency [13].

Recently, In_2O_3 nanowires-based FETs have been demonstrated as a sensitive chemical sensor for NO_2 and NH_3 [14]. In_2O_3 functions as the n-type semiconductor as a result of oxygen vacancy doping [15]. The level of doping is inversely related to oxygen concentration. When an oxygen vacancy is present, a vacancy level appears in the band gap. The vacancy level is composed of In-5 sp orbital hybridized with O-2p orbital which exhibits a strong In–In interaction. Occupation of electrons to the oxygen vacancy results in a stronger In–In bonding strength. Thus, the change in In_2O_3 conductance is due to the electron transfer between the nanowire and the target molecules.

In this context, the redox property of LDL cholesterol permits the nanosensors to accumulate or deplete electrons. The individual LDL cholesterol is approximately 22 nm in diameter with a molecular weight of 2300 kDa (kilo-Dalton). The LDL cholesterol contains an Apo B-100 lipoprotein (550 kDa) [16] which is distinct from high density lipoprotein (HDL). The Apo B-100 lipoprotein contains lysine residues which undergo oxidation in blood or arterial walls; thereby, converting reduced state of LDL (nLDL) to the oxidate state (oxLDL) (Fig. 1). These oxLDL particles trigger vascular oxidative stress and recruitment of inflammatory cells into the vessel walls. The transmigration of these cells, specifically, monocytes, from blood into arterial walls is a crucial event in initiating coronary artery disease [17]. Therefore, the level of circulating oxLDL in human plasma is considered as an emergent marker to predict acute coronary syndromes.

We hereby investigated the effects of reduced nLDL and oxidized LDL cholesterol on the conductivities of In_2O_3 nanowires and carbon nanotubes. The LDL sample containing 15.1% oxLDL particles increased the conductance of the n-type In_2O_3 nanowire-based FET relative to the sample containing 4.4% oxLDL as demonstrated by the current versus drain-source voltage (I_D–V_{DS}) and current versus gate-source voltage (I_D–V_{GS}) plots and validated by high performance liquid chromatography. The identical LDL samples were exposed to the p-type carbon nanotube network. The LDL sample containing 15.1% oxLDL particles decreased the conductance of the p-type carbon nanotube network relative to the sample containing 4.4% oxLDL, demonstrating a complementary response by the $I_D - V_{DS}$ [18]. Furthermore, the carbon nanotube network-based FETs were conjugated with anti-copper oxLDL antibodies and were exposed to the LDL samples in the presence of bovine serum albumin (BSA), a ubiquitous protein carrier in the blood. The LDL sample containing 15.1% oxLDL particles demonstrated high peaks in the I_D versus time plot. Despite the high sensitivity of nanowire-based FETs [19]; device-to-device variations exist among individual transistors. The development and application of high density carbon nanotube network-based FETs which were conjugated with antibodies spe-
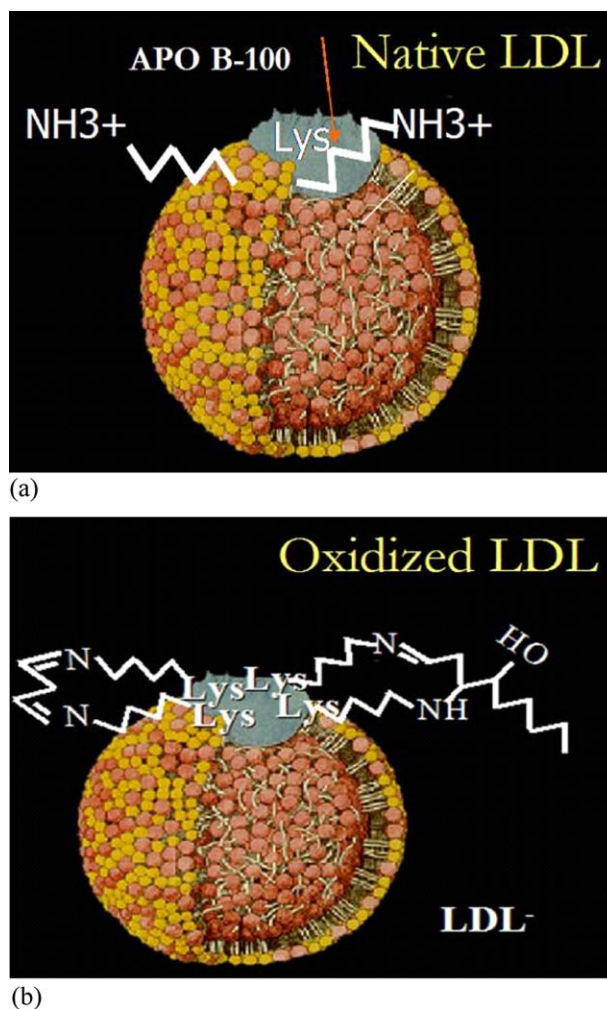

(a)

(b)

Fig. 1. Native vs. oxidized LDL particles. (a) Native LDL represents ~95% of total LDL particles. Oxidative modification of LDL involves alterations in both the protein and lipid components of the LDL particles. Progressive oxidation of the apoprotein is associated with the loss of specific amino acid residues sensitive to oxidation, such as lysine, tyrosine and cysteine [28]. (b) OxLDL or LDL⁻, which is found in plasma in vivo, is characterized by its electronegativity and oxidative status [6]. OxLDL represents 0.2–8% of total LDL particles, and is strongly associated with an increased risk of atherosclerosis [29]. Three possible sources of oxLDL are: (1) oxidation of LDL trapped in the arterial wall; (2) ingestion of oxidants or generation from postprandial lipoprotein remnants [30]; and (3) oxidation in plasma [31].

cific for oxLDL enhanced the selective detection of oxLDL cholesterol.

2. Materials and methods

Bovine serum albumin and methoxypolyethylene glycol imidazolyl carbonyl were purchased from Sigma–Aldrich. Copper-induced oxLDL antibodies were purchased from Biodesign Co, MA. LDL samples were obtained from fasting adult human volunteers under institutional review board approval at the University of Southern California Atherosclerosis Research Unit, Department of Medicine.

2.1. Preparation of LDL

Plasma was obtained from the venous blood, and was pooled and immediately separated by centrifugation at $1500 \times g$ for 10 min at $4\,^\circ$C. LDL ($\delta = 1.019$–1.063 g/mL) was isolated from freshly separated plasma by preparative ultracentrifugation using a Beckman L8-55 ultracentrifuge and a SW-41 rotor. The technique used for separating LDL was similar to that described previously [20]. The isolated LDL was extensively dialyzed against argon-sparged 0.01 M tris–buffer, pH 7.2, containing 100 μM EDTA, sterilized by filtration (0.2 μm Millipore membrane) and stored at $4\,^\circ$C under nitrogen. The LDL fraction was dialyzed and concentrated using a centrifugal filter device (Millipore Corporation, MA) with a molecular weight cut off at 30 kDa. LDL (1 mg protein/mL) in phosphate buffered saline (PBS) containing 100 μM EDTA which was sterilized by filtration through 0.2 μm syringe filter (Corning Corporation, NY) and stored at $4\,^\circ$C until used for various experiments. Protein concentrations were measured by the Bio-Rad protein assay reagent (Bio-Rad, CA) using bovine serum albumin as a standard. Analysis of oxidized LDL in terms of LDL^- and LDL^{2-} was used as a measurement of LDL modification according to the previously described methods [21].

LDL^- and LDL^{2-} are found in plasma in vivo. LDL^- particles are minimally oxidized subspecies of LDL, characterized by their electro-negativity and oxidative status [21]. LDL^- particles are predominantly found in the small dense LDL fraction, and they are strongly associated with an increased risk of atherosclerosis [21,22]. LDL^{2-} particles are more electronegative than LDL^-, and they appear to be highly oxidized sub-fractions of LDL [21].

2.2. Separation of LDL subspecies by HPLC

Native versus oxidized LDL particles were analyzed according to the previously described methods [17]. Briefly, aliquots of LDL (in PBS) isolated from the culture medium at 4 h were subjected to an anion exchange high performance liquid chromatography (Perkin-Elmer). The total LDL was eluted through a UNO-Q1 anion exchange column (BioRad) at 1.0 mL/min and the eluent monitored at 280 nm. Accordingly, the ratios of oxidized LDL relative to total LDL were compared. The proportion of oxidized LDL relative to total LDL was a measure of LDL modification.

2.3. Fabrication of indium oxide nanowire-based field effect transistors

Indium oxide nanowires were synthesized by using the laser ablation process [22]. To achieve a controllable diameter nanowire, a Si/SiO$_2$ substrate, decorated with 10 nm monodispersed gold nanoparticles, was placed downstream of the furnace and the target, InAs, was placed upstream. During laser ablation, a constant flow of 150 standard cubic centimeters per minute (sccm) of argon mixed with 0.02%

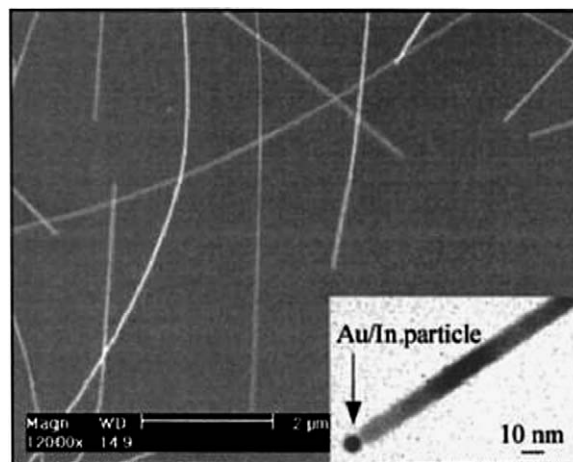Fig. 2. Scanning electron microscopy (SEM) of In$_2$O$_3$ nanowires. Nanowires were synthesized by laser ablation on a Si/SiO$_2$ substrate using monodispersed 10 nm gold clusters as the catalyst. The insert is a tunneling electron microscopy (TEM) of an In$_2$O$_3$ nanowire with a catalyst particle at the tip. The scale bar corresponds to 10 nm.

O$_2$ was introduced into the chamber. Indium vapor, made from laser ablation, alloyed with gold particles through vapour–liquid–solid mechanism. At $770\,^\circ$C in the quartz tube, super saturation developed and single crystalline In$_2$O$_3$ were grown in the presence of the gold catalyst by reacting with oxygen (Fig. 2). To make In$_2$O$_3$-nanowire FETs, we sonicated these nanowires from the silicon substrate suspended in isopropyl alcohol, followed by depositing them onto a degenerately doped silicon wafer coated with 500 nm SiO$_2$. Photolithography and successive Ti/Au deposition were applied to pattern the source and drain electrodes and to establish contact with the individual nanowires (Fig. 3).

## 2.4. Fabricating the microfluidic testing channels

Polydimethylsiloxane (PDMS) elastomer is widely used in microfluidic applications to form components such as channels, valves and diaphragms [23,24] (Sylgard 184 kit; Dow Corning). By using SU8-50 negative photoresist as a molding master, we fabricated the PDMS channels at $360\,\mu$m $\times$ $100\,\mu$m $\times$ 2 mm. The silicon wafers with the nanowires or nanotubes formed the floor of the channels. Target molecules were injected into the channels via a syringe pump (Harvard Apparatus) while the conductivities were measured via the source and drain electrodes patterned at a distance from fluid exposure (Fig. 4).

2.5. Nanotube network transistors

Despite superior sensitivity to detect individual electron transfer [19]; device-to-device variations exist among individual nanowire-based FETs. High density carbon nanotube network-based FETs were fabricated by increasing the catalyst concentration (monodispersed 10 nm iron clusters). Nano-scale iron particles were deposited onto a patterned
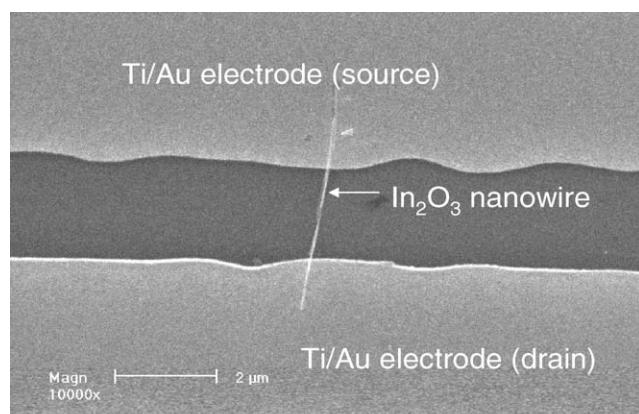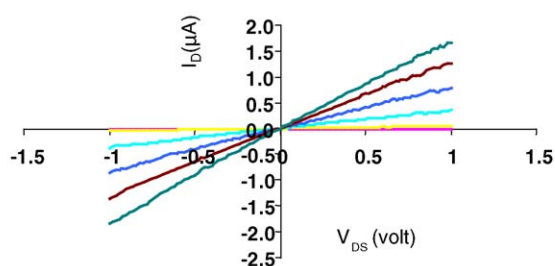
Fig. 3. In$_2$O$_3$ nanowires. (a) After laser ablation synthesis, the In$_2$O$_3$ nanowires were deposited onto a Si/SiO$_2$ substrate by spin coating from a suspension. E-beam lithography or photolithography was used to pattern the source/drain electrodes, followed by deposition and lift-off of Ti/Au to contact individual nanowires. The Si substrate was used as a back gate. (b) I–V_{DS} curves of the device at room temperature: by varying the gate voltage from −5 to 25 V, the conductance of the nanowire was gradually suppressed. This behavior was in agreement with the well-known fact that In$_2$O$_3$ is an n-type semiconductor due to O$_2$ deficiency [15,32].

Si/SiO$_2$ substrate, which allowed single wall nanotubes to grow at 900 °C in the presence of CH$_4$ as the feeding gas [25]. The individual transistors contained multiple nanotubes functioning as the conductive channel between the drains and sources at 500 μm apart from each others. As a result, the overall transistor and sensing characteristics were averaged over an ensemble of nanotubes to reduce device-to-device variations.

2.6. Nanotube network transistors with anti-oxLDL antibodies

The surface of nanotube transistors was coated with a layer of methoxypolyethylene glycol imidazolyl carbonyl (PEG-PEI) (Sigma–Aldrich), a linker layer between the silicon substrate and anti-oxLDL. This coating provided an increase in the binding affinity of carboxyl terminals at the Fc regions of the anti-oxLDL antibodies with the substrate and reduced non-specific binding with non-anti-oxLDL antibodies (Fig. 5a and b). Then, the surface of a network of carbon nanotubes was conjugated with the polyclonal rabbit antibodies specific for copper-induced oxLDL (Biodesign, ME).
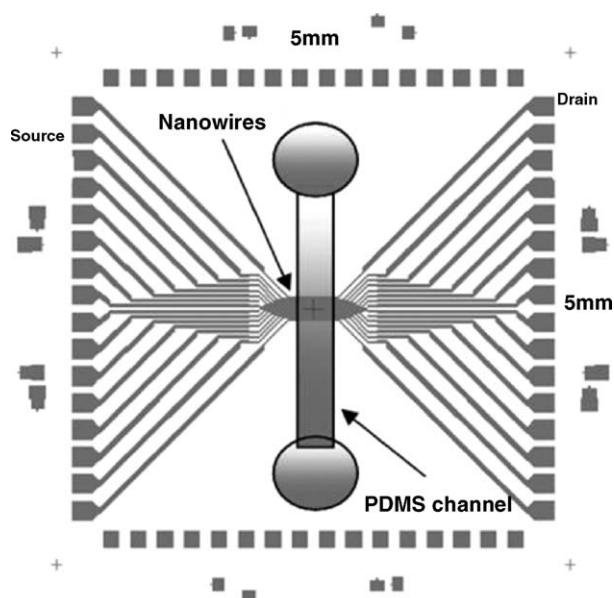

Fig. 4. Electrodes were chosen as source and drain wherever their connection through the nanowire was established. A PDMS channel was designed to cover the area where the nanowires exist to provide the exposure of biomolecules with the nanowires.

This anti-oxLDL antibody provided selectivity for oxLDL particles in the presence of bovine serum albumin. These transistors on the silicon wafers formed the floor of the PDMS channel (Fig. 5c).

3. Experimental protocols

3.1. Individual nanowire-based FETs

The presence of oxLDL in the LDL samples was analyzed by high performance liquid chromatography. The first sample contained 15.1% of oxidized LDL suspended in DI water. The second sample contained 4.4% of oxLDL. We pipetted 0.02 μL of the LDL particles at 0.1 M to the nanowire-based FETs. FET transistor characteristics were analyzed in terms of I–V_{DS} and I–V_{GS} of the FETs (Agilent 4156B Semiconductor parameter analyzer). The baseline I–V_{DS} and I–V_{GS} were calibrated in the presence of DI water. The conductivities of FET depended on whether the energy level of water was above or below the FET's Fermi level. The LDL samples exposed to two individual nanowire-based FETs.

3.2. Nanotube network-based FETs

The copper-induced oxLDL particles at 200 μg/mL were introduced to the PDMS channel which housed the nanotubes conjugated with copper-induced oxLDL antibodies. Conductivity curve was constructed by using a lock-in amplifier (SR810, Stanford Research Systems) to improve the signal to noise ratio. BSA (Sigma–Aldrich) at 200 μg/mL was introduced, followed by introduction of native LDL and water. Changes in conductivity were monitored.
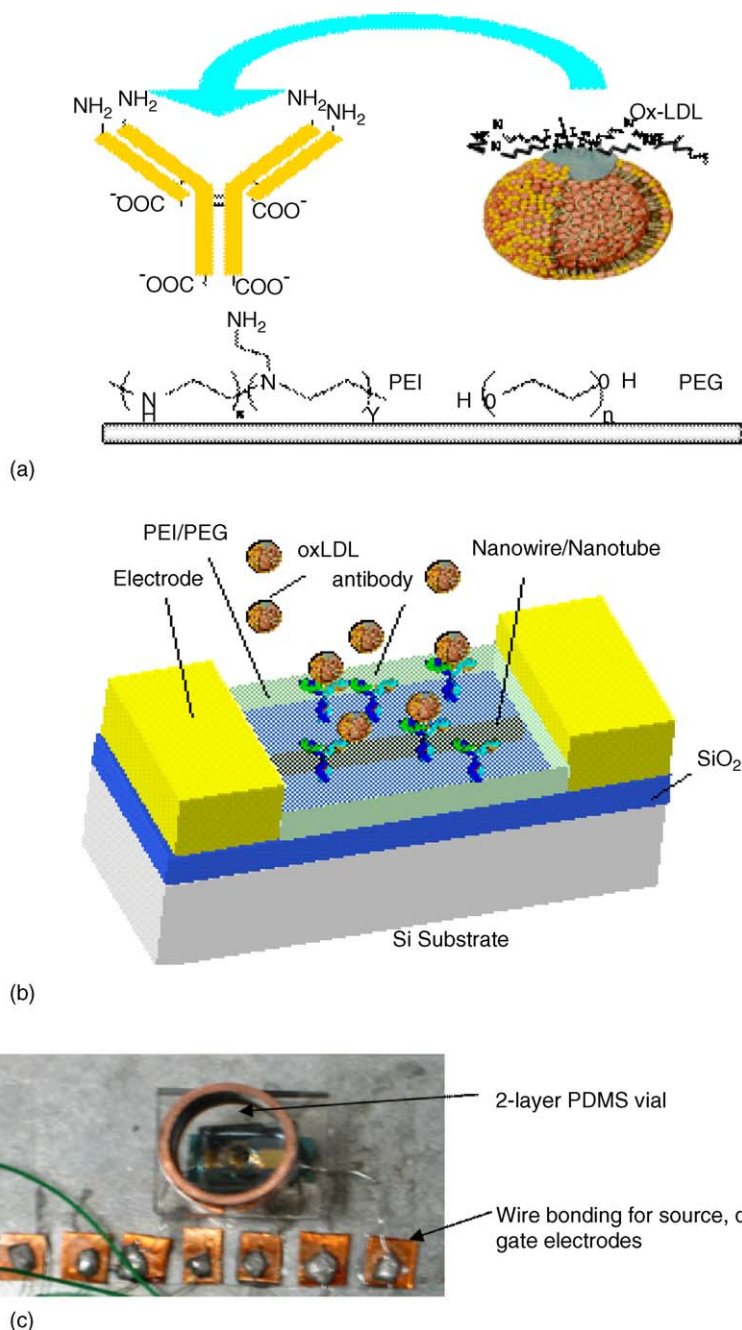
Fig. 5. Surface functionalization. (a) Surface chemistry modification was performed to the nanowire for selective detection of oxLDL. The copper-induced anti-oxLDL antibodies were conjugated to the nanowires via a linker layer of methoxypolyethylene glycol imidazolyl carbonyl. (b) A three-dimensional configuration of a functionalized FET. (c) A PDMS channel houses the nanowire network FETs.

4. Results

4.1. The extent of LDL oxidation by HPLC

The LDL samples from human plasma were analyzed for the extent of LDL oxidization by HPLC (Fig. 6). The major fraction of the LDL particles was nLDL as shown in Fig. 6a. The fraction of oxLDL was shown as two smaller peaks in terms of LDL^- and LDL^{2-}, respectively. In sample 1, the total oxidized LDL was at 4.4%, consisting of LDL^- at 2.9%

and LDL^{2-} at 1.5% (Fig. 6a). In sample 2, the total oxidized LDL was at 15.1%, consisting of LDL^- at 12.9% and LDL^{2-} at 2.2% (Fig. 6b).

4.2. The extent of LDL oxidation corresponded to distinct conductivity by nanowire-based FETs

The FET conductivities characterized by I–V_{DS} and I–V_{GS} curves were compared between the two samples. DI water was pippetted to the nano device to establish baseline. A
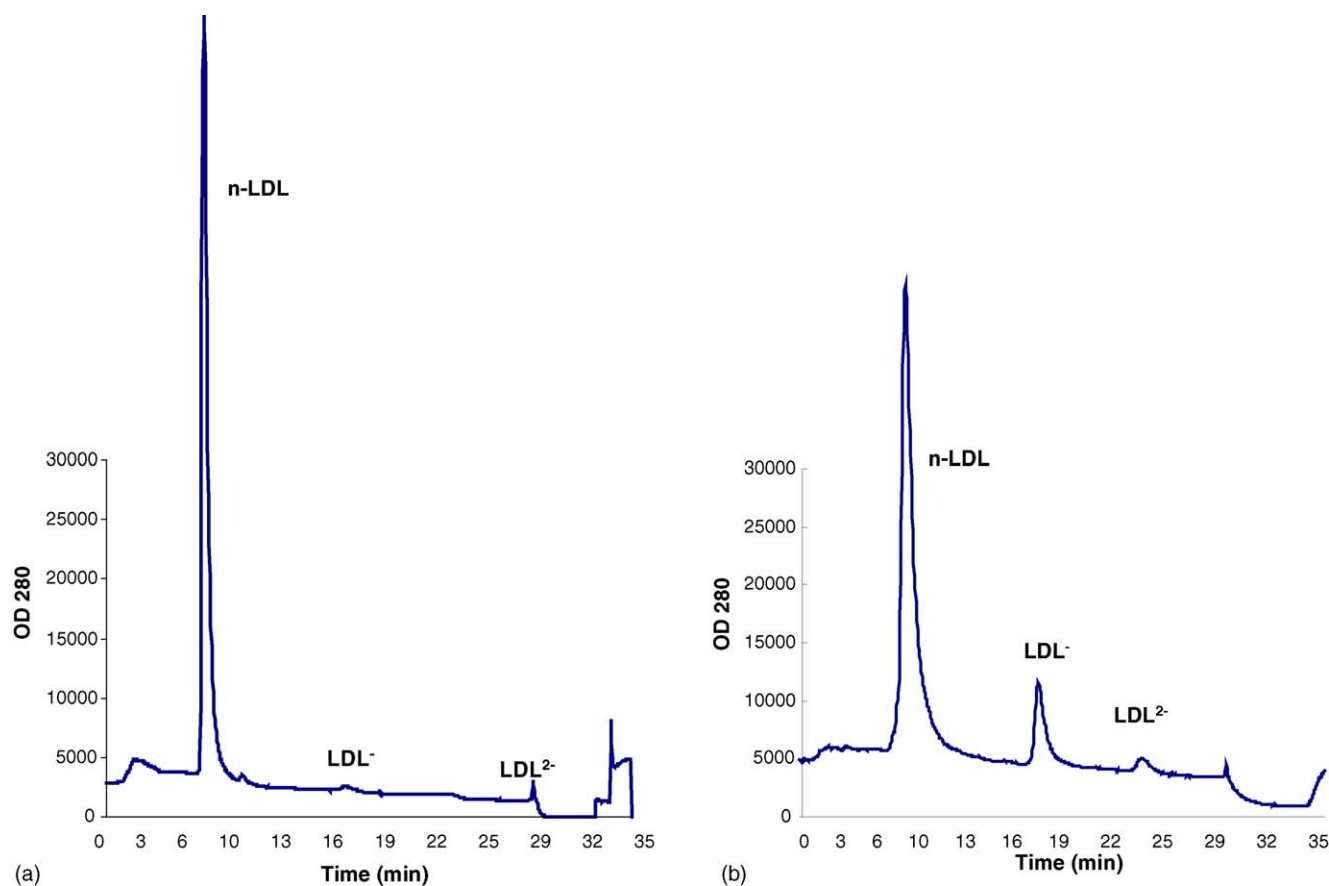
Fig. 6. HPLC chromatograms of LDL particles isolated from human plasma. (a) Three peaks corresponded to nLDL, the most abundant fraction, followed by LDL$^-$ and LDL^{2-}. The LDL sample contained 4.4% of oxLDL, including 2.9% of LDL$^-$ and 1.5% of LDL^{2-}. (b) The LDL sample contained 15.1% of oxLDL; including 12.9% of LDL^{-1} and 2.2% of LDL^{2-}.

very small change in conductivity was observed in the presence of DI water; however, exposing nanowires to LDL particles at different degrees of oxidation resulted in a significant change in conductivities. The LDL sample containing 15.1% oxidized LDL induced a higher level of conductivity than the one containing 4.4%, suggesting an increase in the FET carrier concentration (Fig. 7). I–V_{DS} curve showed the conductivity at 3 μS in the presence of 15.1% oxLDL and at 0.45 μS in the presence of 4.4% oxLDL.

4.3. The extent of LDL oxidation induced a different level of threshold voltage for the nanowire-based FET

Threshold voltage represented the voltage at which the FET was switched from a blocking (off) state to a conducting (on) state. In response to the LDL particles, FET threshold voltage was reduced to a more negative value as demonstrated in the I–V_{GS} curve. The nanowire-based FET was switched to a conducting state earlier than the initial state prior to LDL exposure (Fig. 8). We observed that the sample containing 4.4% oxLDL induced a more negative shift in the threshold voltage compared with the sample containing 15.1% oxLDL (Fig. 8a and b).

LDL particles induced a greater extent of hysteresis than the initial state (Fig. 8a and b) as evidenced by the double-sweeping I–V_{GS} curve at 1 V/s. This observation suggests a substantially weakened gate effect as a result of the LDL particles attached to the nanowires forming charge traps. A similar phenomenon has also been reported in detecting NH$_3$ by using In$_2$O$_3$ nanowires [26].

4.4. Time-dependent responses

The nanowire-based conductivity modulation over time was performed in terms of current versus time curves. Introduction of the LDL particles immediately increased the FET conductivity that remained for 2000 s (Fig. 9). The sample containing 15.1% of oxLDL gave rise to a constant current at 0.6 μA (Fig. 9a) while the sample containing 4.4% of oxidized LDL gave rise to a lower current level (Fig. 9b). This observation was consistent with the trends in terms of I–V_{DS} curves (Fig. 7a and b).

4.5. I–V_{DS} curves between nLDL and oxLDL

I–V_{DS} curve of FET showed a distinct difference in the conductivity between samples containing 15.1% of oxidized

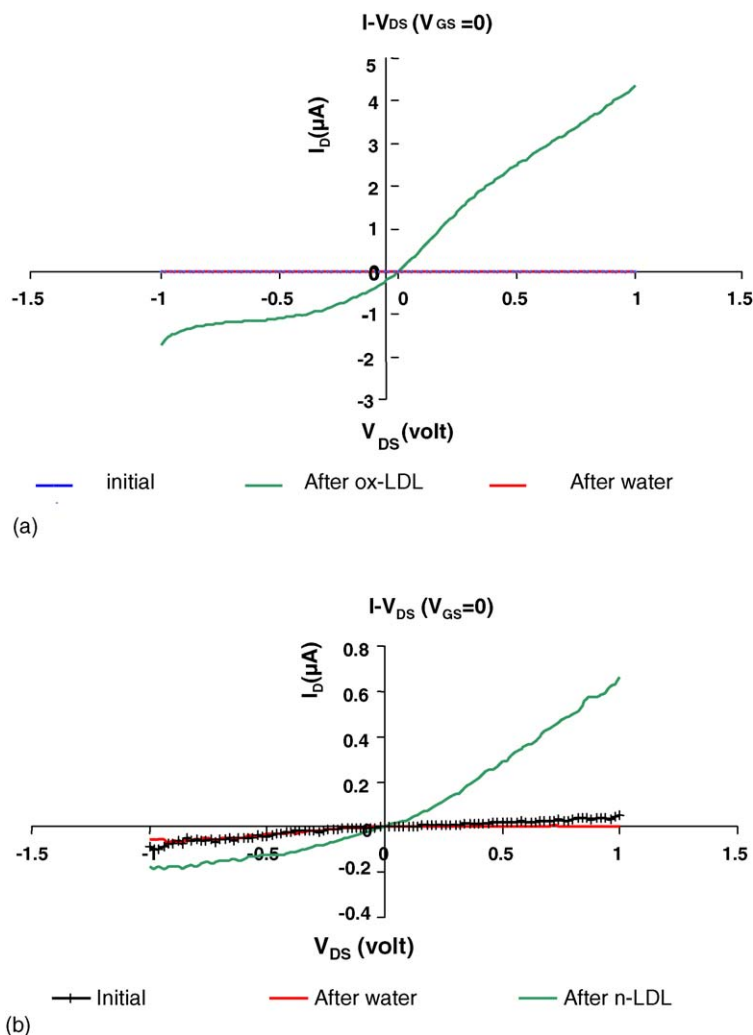Fig. 7. I–V_{DS} curve. (a) OxLDL gave rise to an increase in conductivity compared to the initial state and water. I–V_{DS} curve was biased at zero gate voltage. (b) Native LDL generated a smaller degree of increase in conductivity compared to oxLDL.

LDL and 4.4% of oxidized LDL (Fig. 10). The initial conductivity (in black) was lower than that of native LDL (sample 2: 4.4% of oxLDL, 95.5% of nLDL) (in blue). Oxidized LDL (sample 1: 15.1% oxLDL) significantly increased the conductivity by five-fold.

4.6. Detection of oxLDL by the nanotube network-based FETs

Carbon nanotube network FETs functionalized with methoxypolyethylene glycol imidazolyl carbonyl and copper-induced anti-oxLDL antibodies were used to detect conductivities upon exposure to LDL particles in the presence of BSA. OxLDL increased the conductivity by five-fold (Fig. 11). However, BSA decreased the conductivity. Re-exposure to oxLDL restored the conductivity. This trend was reproducible with repeated trials, suggesting that nanotube network-based FETs were able to selectively detect oxLDL from the non-redox protein, BSA.

5. Discussion

In$_2$O$_3$ nanowire- and carbon nanotube-based FETs provide a new venue to differentiate LDL cholesterol between the reduced and oxidized states. To our best knowledge, applications of nanosensors to detect oxLDL have not previously been demonstrated. The results were validated by HPLC as the gold standard to fractionate LDL particles. The nanowire- and nanotube-based FETs usher in a potential lab-on-a-chip platform to predict acute coronary syndromes at a small quantity of samples from the patients' plasma.

Electron transfer from oxLDL particles to the In$_2$O$_3$ nanowire changed the level of FET's conductivity. This phenomenon can be described by the concept of energy bands (Fig. 12). Two energy band diagrams are illustrated with E_c, E_v and E_f, corresponding to the conduction band, the valence band and the Fermi level of In$_2$O$_3$ nanowires. A proposed energy level denoted as E_{LDL} represents the electrical potential of the electrons that participate in the electron transfer
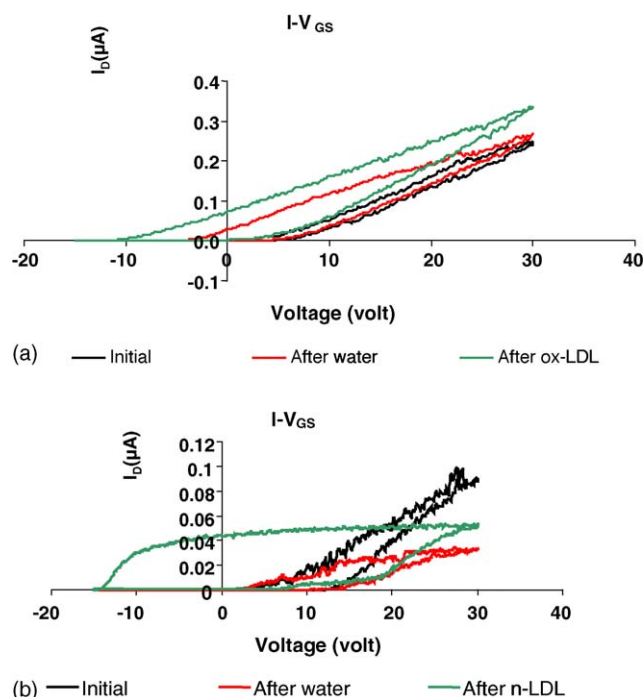
Fig. 10. $I–V_{DS}$ selectivity curve under dynamic condition. The presence of oxLDL (15.1%) gave rise to the highest conductivity compared with nLDL (4.4%).

Fig. 11. Time-domain plot based on the functionalized nanotube network. Upon exposure to oxLDL (15.1%) at 1200 and 1800 s, respectively, the conductivity increased by five-fold. Introduction of BSA at 2300 s decreased the conductivity. Conductivity remained unchanged after introduction of water at 2600 s. Native LDL (4.4%) increased the conductivity at a lower extent compare to oxLDL. The exposure of oxLDL at 4000 s restored the trend in conductivity.

process. The energy levels for LDL particles are located at higher level than the Fermi level, largely due to the charges present in amino acid residues of the ApoB-100. The sample containing 15.1% of oxLDL generated a higher energy level, and hence, a higher degree of conductivity.

Carbon nanotube network-based FETs were investigated for selectivity rather than In_2O_3 nanowires for the following reasons: (1) both In_2O_3 nanowire field effect transistors and carbon nanotube field effect transistors (FET) have shown complementary characteristics in response to exposure to low density lipoproteins (LDL); (2) carbon nanotubes are hydrophobic while In_2O_3 nanowires are hydrophilic. In this context, the methoxypolyethylene glycol imidazolyl carbonyl (PEG-PEI), a linker layer, displayed a stronger bind-

Fig. 8. (a) OxLDL gave rise to a negative shift in threshold voltage accompanied with a larger degree of hysteresis compared to the initial state. The double sweep measurement of $I–V_{GS}$ curve was biased at $V_{DS} = -0.1$ V. (b) Native LDL gave rise to a larger negative shift in threshold voltage and hysteresis.
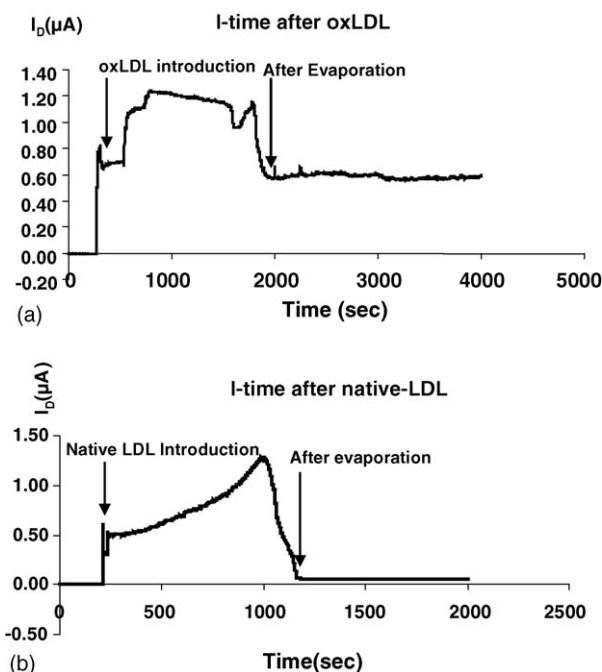

Fig. 9. (a) Time-domain plot illustrated FET conductivity upon exposure to oxLDL sample (containing 15.1% of oxLDL). A change in FET conductivity occurred as a result of water evaporation at time 1800 s. (b) Time-domain plot upon exposure to native LDL samples (containing only 4.4% oxLDL). A change in conductivity occurred as a result of water evaporation at time: 1000 s.
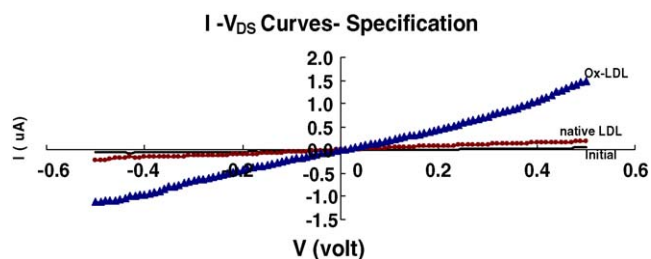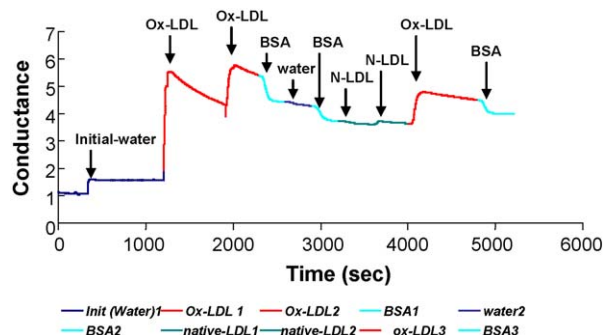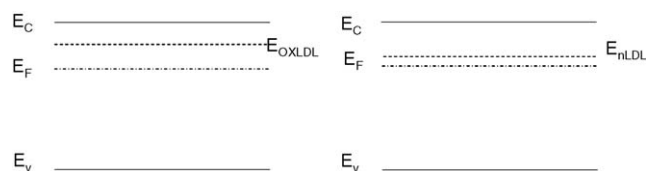

Fig. 12. E_c, E_v and E_f correspond to the conduction band, the valence band and the Fermi level of In_2O_3 nanowires, respectively. A proposed energy level denoted as E_{LDL} represents the electrical potential that participate in the electron transfer process.
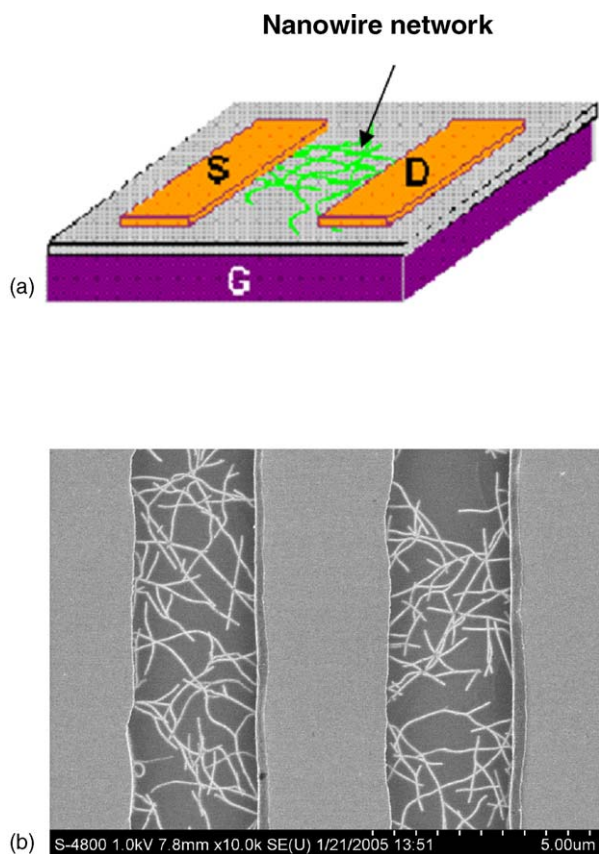
Nanowire network

Fig. 13. (a) Nanowire network devices consist of a matrix of synthesized nanotubes contacted by source (S), drain (D) electrodes and gate (G). (b) SEM photo of carbon nanotube network (drain and source electrodes are not shown in this range).

ing affinity to the nanotube-based FETs than to the In_2O_3 nanowires; (3) carbon nanotubes were fabricated in a network fashion (Fig. 13). Selectivity was achieved by functionalization of individual sensors in the entire network. This enhanced the signal to noise ratio as well as the selectivity. The individual transistors contained multiple nanotubes functioning as the conductive channel between the drains and sources. As a result, the overall transistor and sensing characteristics were averaged over an ensemble of nanotubes to reduce device-to-device variations. Despite the trade off in sensitivity, the combination of nanotube network and surface functionalization with specific anti-oxLDL favored the investigation of selectivity using carbon nanotube network.

Two possible factors accounted for the increased electron concentration in the nanowires: (1) the amino groups carried by the ApoB-100 protein in LDL particles functioned as reductive species by donating electrons to the nanowires; and (2) positive charges carried by the amino groups functioned as a positive gate bias to the nanowires, leading to an enhanced carrier concentration. In both samples, the amino groups in the Apo-B100 portion of the native LDL particles carried positive charges (Fig. 1). The positive charges influenced FETs to the same degree as applying positive gate voltage to turn on the n-type transistor at a lower threshold voltage. In the case of oxLDL, the positive charges in the amino groups were replaced by the hydroxyl group [27].

Individual nanowire transistors exhibit device-to-device variations. To gain the fabrication consistency, we have tested carbon nanotube networks as shown in Fig. 13. Such a network allowed for a multitude of conducting channels between source and drain in the FET configurations. The network-based FETs provided two advantages: (1) the architecture is fault tolerant; that is, the dysfunction of one channel still allows for other channels open for the conduction pathway between source and drain; and (2) the large number of nanowires provides statistical averaging and identical overall nanowire density. Using the carbon nanotubes network conjugated with anti-oxLDL antibodies, we were able to reproduce the conductivities upon exposure to oxLDL samples in the presence of BSA. Future efforts will be to optimize the In_2O_3 nanowire network by balancing the fabrication consistency and the device performance.

While the majority of literatures for nano-sensing have been conducted in the vacuum condition to achieve a high signal to noise ratio, we demonstrate the possibilities of detecting oxLDL under the liquid condition. Furthermore, functionalization of the nanotube network provided an entry point toward detection of oxLDL in the presence of non-redox BSA.

6. Conclusion

Our study demonstrates that In_2O_3 nanowire-based FET represents a potential sensor for detecting redox proteins such as oxLDL particles. Our data supported the possibility of distinguishing the LDL sample containing oxLDL from that of nLDL via the changes in nanowire-based FET conductivity and threshold voltages. Using both the $I_D–V_{DS}$ and $I_D–V_{GS}$ plots, we showed that the sample containing higher level of oxLDL particles increased the conductivity to a greater extent than the one containing lower level of oxLDL.

References

[1] C.J. Murray, A.D. Lopez, Alternative projections of mortality and disability by cause 1990–2020: Global Burden of Disease Study Lancet. 1997 May 24 349 (9064) 1498–1504.

[2] M. Navab, A.M. Fogelman, J.A. Berliner, M.C. Territo, L.L. Demer, J.S. Frank, A.D. Watson, et al., Pathogenesis of atherosclerosis, Am. J. Cardiol. 76 (1995) 18C–23C.

[3] M.S. Penn, M.Z. Cui, A.L. Winokur, et al., Smooth muscle cell surface tissue factor pathway activation by oxidized low-density lipoprotein requires cellular lipid peroxidation, Blood 96 (9) (2000) 3056–3063.

[4] M.A. Austin, Small, dense low-density lipoprotein as a risk factor for coronary heart disease, Int. J. Clin. Lab. Res. 24 (4) (1994) 187–192.

[5] S. Ehara, M. Ueda, T. Naruko, K. Haze, A. Itoh, M. Otsuka, R. Komatsu, T. Matsuo, et al., Elevated levels of oxidized low density lipoprotein show a positive relationship with the severity of acute coronary syndromes, Circulation 103 (15) (2001) 1955–1960.

[6] A. Sevanian, H. Hodis, Antioxidants and atherosclerosis: an overview, Biofactors 6 (1997) 385–390.

[7] Supriyo Bandyopadhyay, Hari Singh Nalwa, Quantum Dots and nanowires, American Scientific publishers, p. 193.

[8] R.L. Weiher, R.P. Ley, J. Appl. Phys. 37 (1966) 299.

[9] G. Rupprecht, Z. Phys. 139 (1954) 504.

[10] Zu Rong Dai, Zhong Lin Wang, Nanobelts of Semiconcting Oxides, Science, vol. 291, 2001, p. 1947.

[11] J. Kong, N. Franklin, C. Zhou, S. Peng, K. Cho, H. Dai, Nanotube molecular wires as chemical sensors, Science 287 (2000) 622.

[12] Q. Yi Cui, W. Hongkun Park, M. Charles, Lieber, Nanowire nanosensors for highly sensitive and selective detection of biological and chemical species, Science 293 (2001) 1289–1292.

[13] D.S. Ginley, C. Bright, Bull. Mater. Res. Soc. 25 (2000) 15.

[14] C. Li, D. Zhang, X. Liu, S. Han, T. Tang, J. Han, C. Zhou, In_2O_3 nanowires as chemical sensors, Appl. Phys. Lett. 82 (2003) 1613.

[15] J.R. Bellingham, A.P. Mackenzie, W.A. Philips, Transparent conducting thin films: precise measurement of the oxygen content, Appl. Phys. Lett. 58 (1991) 2506.

[16] Lubert Stryer, Biochemistry, third edition, W.H. Freeman and company, p. 561.

[17] T. Henriksen, E.M. Mahoney, D. Steinberg, Enhanced macrophage degradation of low density lipoprotein previously incubated with cultured endothelial cells: recognition by receptors for acetylated low density lipoproteins, Proc. Natl. Acad. Sci. U.S.A. 78 (10) (1981) 6499–6503.

[18] T. Tang, X. Liu, C. Li, B. Lei, D. Zhang, M. Rouhanizadeh, T. Hsiai, C. Zhou, Complementary response of In_2O_3 nanowires and carbon nanotubes to low-density lipoprotein chemical gating, Appl. Phys. Lett. (2005) 86.

[19] C. Li, B. lei, D. Zhang, X. Liu, S. Han, T. Tang, M. Rouhanizadeh, T. Hsiai, C. Zhou, Chemical gating of In_2O_3 nanowires by organic and biomolecules, Appl. Phys. Lett. (2003) 4014–4016.

[20] H.N. Hodis, D.M. Kramsch, P. Avogaro, G. Bittolo-Bon, G. Cazzolato, J. Hwang, H. Peterson, A. Sevanian, Biochemical and cytotoxic characteristics of an in vivo circulating oxidized low density lipoprotein (LDL-), J. Lipid Res. 35 (1994) 669–677.

[21] J. Hwang, M. Ing, A. Salazar, M. Navab, A. Sevanian, T. Hsiai, Pulsatlile versus oscillatory shear stress regulates NADPH oxidase subunit: implication for native LDL oxidation, Circ. Res. 93 (12) (2003) 1225–1232, Epub 2003 October 30, December 12.

[22] C. Li, D. Zhang, S. Han, X. Liu, T. Tang, C. Zhou, Diameter-controlled growth of single-crystalline In_2O_3 nanowires and their electronic properties, Adv. Mater. 15 (2003) 143.

[23] B.-H. Jo, L.M. Van Lerberghe, K.M. Motsegood, D.J. Beebe, Three dimensional micro-channel fabrication in PDMS elastomer, J. MEMS 9 (2000) 76–81.

[24] A. Unger, H.-P. Chou, T. Thorsen, A. Scherer, S.R. Quake, Monolithic microfabricated valves and pumps by multilayer soft lithography, Science 288 (2000) 113–116.

[25] X. Liu, C. Lee, C. Zhou, J. Han, Carbon nanotube field effect inverters, Appl. Phys. Lett. 79 (20) (2001) 3329–3331, November 12.

[26] D. Zhang, C. Li, X. Liu, S. Han, T. Tang, C. Zhou, Doping-dependent ammonia sensing of indium oxide nanowires, Appl. Phys. Lett. 84 (No. 9) (2003) 1845.

[27] A. Sevanian, L. Asatryan, O. Ziouzenkova, Low density lipoprotein (LDL) modification: basic concepts and relationship to atherosclerosis, Blood Purif. 17 (1999) 66–78.

[28] A. Sevanian, G. Bittolo-Bon, G. Cazzolato, H. Hodis, J. Hwang, A. Zamburlini, M. Maiorino, F. Ursini, LDL is a lipid hydroperoxide-enriched circulating lipoprotein, J. Lipid Res. 38 (3) (1997) 419–428.

[29] M.A. Austin, Small, dense low-density lipoprotein as a risk factor for coronary heart disease, Int. J. Clin. Lab. Res. 24 (4) (1994) 187–192.

[30] R.B. Wesley Jr, X. Meng, D. Godin, Z.S. Galis, Extracellular matrix modulates macrophage functions characteristic to atheroma: collagen type I enhances acquisition of resident macrophage traits by human peripheral blood monocytes in vitro, Arterioscler. Thromb. Vasc. Biol. 18 (1998) 432–440.

[31] W.L. Stone, M. Heimberg, R.L. Scott, I. LeClair, H.G. Wilcox, Altered hepatic catabolism of low-density lipoprotein subjected to lipid peroxidation in vitro, Biochem. J. 297 (Part 3) (1994) 573–579.

[32] J. Tamaki, C. Naruo, Y. Yamamoto, M. Mastuoka, Sensing properties to dilute chlorine gas of indium oxide based thin film sensors prepared by electron beam evaporation, Sens. Actuators B 83 (190) (2002).

Biographies

Mahsa Rouhanizadeh received her B.S. in Electrical Engineering from Sharif University of Technology, Tehran, Iran in February 1999. She then obtained a DEA in "Information processing for electrical systems" at University of Paris, France in September 2000. Then she continued graduate studies at University of Southern California, Los Angeles where she received M.S. degree in Electrical Engineering in May 2002. She is currently a Ph.D. candidate in the Department of Biomedical Engineering and Division of Cardiovascular Medicine. Her research interests are micro and nano-sensors for diagnosis of cardiovascular diseases. She has been a member of IEEE since 2001.

Tao Tang received B.Sc. degree from Beijing Institute of Technology, China, in 2001, and M.Sc. degree from University of Southern California in 2004. He is currently pursuing Ph.D. degree from Department of Electrical Engineering – Electrophysics at University of Southern California.

Chao Li received her Ph.D. degree from Electrical Engineering department of University of Southern California in 2005. She received her M.Sc. and B.Sc. degrees from Lanzhou University, China, in 2001 and 1998, respectively. Her research interests are the synthesis, electronic studies and applications of nanoscale materials.

Juliana Hwang received Pharm.D. degree from the School of Pharmacy at the University of Sao Paulo, Brazil in 1986. She currently holds a position of Research Assistant Professor at School of Pharmacy at Molecular Pharmacology and Toxicology Department at the University of Southern California. Her research interests are in the area of investigating the manner by which estrogen facilitates the antioxidant capacity of vascular cells and mechanisms by which estrogen decrease the development of atherogenesis in the vessel wall.

Chongwu Zhou received his Ph.D. from Yale University in 1999. He received his B.Sc. from the University of Science and Technology of

China in 1993. He worked as a Postdoctoral Research Assistant at Stanford University from 1998 to 2000. He is currently an Assistant Professor at the Department of Electrical Engineering – Electrophysics of University of Southern California. His research interests are in the areas of carbon nanotubes, semiconductive nanowires, transition metal oxide nanowires, molecular electronics, and chemical and bio sensing. He has won a number of awards including the NSF CAREER Award and the NASA TGiR Award.

Dr. Tzung K. Hsiai received his B.S. from Columbia University and M.D. from the University of Chicago. Dr. Hsiai underwent his postgraduate medical training and NIH NRSA for cardiology fellowship at UCLA School of Medicine, where he obtained a Ph.D. in Biomedical Engineering in 2002. He is recipient of NIH Physician Scientist Career Development Award, and American Heart Association John J. Simpson Outstanding Research Achievement Award. T.K. Hsiai was elected as a Fellow of American College of Cardiology in 2005.